Viscoelastic properties of collagen: synchrotron radiation investigations and structural model

R. Puxkandl[1], **I. Zizak**[1]†, **O. Paris**[1], **J. Keckes**[1], **W. Tesch**[1,2], **S. Bernstorff**[3], **P. Purslow**[4] and **P. Fratzl**[1,2]*

[1]*Erich Schmid Institute of Materials Science, Austrian Academy of Sciences, and University of Leoben, Jahnstrasse 12, 8700 Leoben, Austria*
[2]*Ludwig Boltzmann Institute of Osteology, Hanusch Hospital, Vienna, Austria*
[3]*Sincrotrone Trieste S.C.p.A, SS 14, km 163.5, in Area Science Parc, Basovizza, I-34012 Trieste, Italy*
[4]*Department of Biological Sciences, University of Stirling, Stirling FK9 4LA, UK*

Collagen type I is the most abundant structural protein in tendon, skin and bone, and largely determines the mechanical behaviour of these connective tissues. To obtain a better understanding of the relationship between structure and mechanical properties, tensile tests and synchrotron X-ray scattering have been carried out simultaneously, correlating the mechanical behaviour with changes in the microstructure. Because intermolecular cross-links are thought to have a great influence on the mechanical behaviour of collagen, we also carried out experiments using cross-link-deficient tail-tendon collagen from rats fed with β-APN, in addition to normal controls.

The load–elongation curve of tendon collagen has a characteristic shape with, initially, an increasing slope, corresponding to an increasing stiffness, followed by yielding and then fracture. Cross-link-deficient collagen produces a quite different curve with a marked plateau appearing in some cases, where the length of the tendon increases at constant stress. With the use of *in situ* X-ray diffraction, it was possible to measure simultaneously the elongation of the collagen fibrils inside the tendon and of the tendon as a whole. The overall strain of the tendon was always larger than the strain in the individual fibrils, which demonstrates that some deformation is taking place in the matrix between fibrils. Moreover, the ratio of fibril strain to tendon strain was dependent on the applied strain rate. When the speed of deformation was increased, this ratio increased in normal collagen but generally decreased in cross-link-deficient collagen, correlating to the appearance of a plateau in the force–elongation curve indicating creep.

We proposed a simple structural model, which describes the tendon at a hierarchical level, where fibrils and interfibrillar matrix act as coupled viscoelastic systems. All qualitative features of the strain-rate dependence of both normal and cross-link-deficient collagen can be reproduced within this model. This complements earlier models that considered the next smallest level of hierarchy, describing the deformation of collagen fibrils in terms of changes in their molecular packing.

Keywords: collagen; synchrotron; X-ray; viscolelastic; mechanical properties

1. INTRODUCTION

Tendon is a hierarchically structured collagenous tissue that has outstanding mechanical properties. The stress–strain curve of tendons usually exhibits three distinct regions (Vincent 1990), which can be correlated to deformations at different structural levels. In the first region, at small strains, a very small stress is sufficient to elongate the tendon. This region is sometimes called the toe region and is correlated to the removal of the macroscopic crimp in the collagen fibrils (Diamant *et al.* 1972). In the second region, at higher strains, the stiffness of the tendon increases considerably with the extension. An entropic mechanism, where disordered molecular kinks in the gap region of collagen fibrils are straightened out, has been

proposed to explain the increasing stiffness with increasing strain (Misof *et al.* 1997). When all the kinks are straightened, another mechanism of deformation must prevail and explain the linear dependence of stress and strain in this region of the force–elongation curve. The most probable processes are thought to be the stretching of the collagen triple helices and the cross-links between the helices, implying a side-by-side gliding of neighbouring molecules, leading to structural changes at the level of the collagen fibrils. This has previously been investigated by the use of synchrotron radiation diffraction experiments (Mosler *et al.* 1985; Folkhard *et al.* 1986; Sasaki & Odajima 1996; Fratzl *et al.* 1997; Sasaki *et al.* 1999). By monitoring the structure factors of the second and third order maximum, it was shown that during stretching the length of the gap region was increased with respect to the overlap region, implying a considerable gliding of neighbouring molecules (Folkhard *et al.* 1986; Fratzl *et al.* 1997). Moreover, it was found that the elongation of collagen fibrils (as measured

*Author for correspondence (fratzl@unileoben.ac.at).
† Present address: Hahn-Meitner-Institut, Glienickerstrasse 100, D-14109 Berlin, Germany.

Phil. Trans. R. Soc. Lond. B (2002) **357**, 191–197
DOI 10.1098/rstb.2001.1033

191

by the increase in the axial repeat of the molecular packing of the fibrils) is always considerably less than the total elongation of the tendon (Fratzl *et al.* 1997). Typically, the strain of the fibrils is less than half that in the whole tendon. This emphasizes the fact that the proteoglycan-rich matrix between the fibrils also experiences a considerable deformation (Cribb & Scott 1995). Relatively little is known, however, about the relative importance and the mechanisms of fibril and matrix deformation.

In order to get some insight into the coupling between the deformation in fibrils and in the surrounding matrix, further *in situ* tensile testing and synchrotron X-ray diffraction experiments on rat-tail tendons were carried out. Two approaches were pursued in order to induce differences in the deformation behaviour between fibrils and interfibrillar matrix: first, we varied the strain rate systematically, assuming that the viscosity of fibrils and matrix could be different. Second, we compared normal with cross-link-deficient collagen from rats fed with β-APN. It is well known that the formation of covalent cross-links between adjacent molecules may be inhibited by β-APN (Eyre *et al.* 1984), which acts by the enzymatic process of aldehyde formation (Tang *et al.* 1983; Lees *et al.* 1990). It has also been shown previously that cross-links have a large influence on the mechanical behaviour of collagen; an increased number of cross-links increases its stiffness (Eyre *et al.* 1984; Davison 1989; Bailey *et al.* 1998) (and also brittleness; Light & Bailey (1979)), while a reduction due to β-APN reduces its stiffness dose-dependently (Lees *et al.* 1990).

We further proposed a structural and mechanical model for the interaction between collagen fibrils and interfibrillar matrix, which explains the essentials of the observed effects via calculation of viscoelastic properties within the simplest possible mathematical framework. This model is discussed in conjunction with an earlier proposal for the deformation mechanisms at the next smallest hierarchical level, the collagen fibrils (Fratzl *et al.* 1997).

2. MATERIAL AND METHODS

Native fibres from rat-tail tendons were measured. The tail tendons were obtained from a seven week old rat fed with 0.17 g day^{-1} of β-APN for the last three weeks and from a six week old rat fed with 0.4 g day^{-1} of β-APN for the last three weeks. For comparison, tails from two six week old rats not fed with β-APN were used as a control group. The tails were frozen and stored at *ca.* −18 °C until dissection. After dissection, the tail tendons were immediately stored in PBS at pH 7.4 to prevent deterioration. There was no observable difference in the behaviour of a specimen stored in PBS at 4 °C for several months and a specimen measured directly after dissection (Misof *et al.* 1997).

The mechanical testing was performed with a special device developed for this purpose (Fratzl *et al.* 1997; Misof *et al.* 1997), while time-resolved X-ray diffraction patterns were taken simultaneously, at intervals that depended on the strain rate and lasted between 30 and 50 s. The X-ray diffraction experiments were carried out at the SAXS Beamline of the synchrotron radiation source Elettra in Trieste (Amenitsch *et al.* 1995), because a large X-ray flux was needed to obtain X-ray diffraction patterns of sufficient counting statistics in such a short measuring time. The data were collected using a two-dimensional position
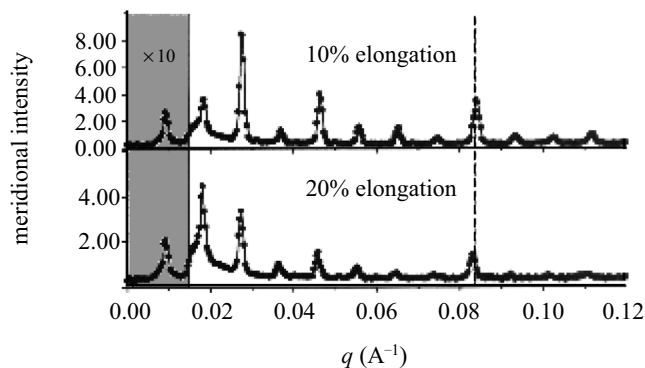

Figure 1. The evolution of the axial (meridional) diffraction peaks with the macroscopic elongation. The peaks arise from the periodic arrangement of collagen molecules within fibrils (Hodge & Petruska 1963). The period, *D*, was evaluated by fitting the peak positions using Gaussian functions for each peak. Peak positions are clearly seen to lie at smaller *q* values (longer real spacings) at the higher extensions.

sensitive X-ray CCD camera (AXS, Karlsruhe). The first 12 reflections of the axial period of the collagen fibrils were recorded. A simultaneous fit of all peak positions (weighted with the intensity of the peaks to improve statistical accuracy) yielded the axial repeat, *D* (figure 1).

At the same time, the macroscopic strain in the whole tendon was determined by the movement of the clamps holding the tendon and the applied load measured by a force sensor. The tendons were kept partially immersed in PBS during the whole experiment to avoid drying. Each experiment was carried out at a constant velocity of elongation, which was chosen to be between 0.0001 and 0.01 mm s^{-1} for the control group and between 0.0001 and 0.005 mm s^{-1} for the two β-APN-treated rats. Each tendon was stretched to failure and a load–extension curve was recorded. The initial length of the fibre was determined by stretching it until the smallest force (0.005 N) was detected. The fibre length at this load was then taken as the initial length. By correlating the time from the start of each tensile test, the structural information contained in the diffraction patterns (that is, the *D*-period of the fibrils) could be matched with the corresponding point on the load–extension curve.

3. RESULTS

Typical load–elongation curves for three different types of samples can be seen in figure 2. It is readily seen that all three curves show a similar behaviour in the first part of the plot at low strains. All samples developed a toe region, a heel region and a linear region, although the corresponding macroscopic strains were slightly lower for tendons taken from the β-APN-treated rats.

Figure 2*a* shows the typical curve for normal collagen. Twelve of the 20 tendons from β-APN-treated rats demonstrated a distinctive mechanical behaviour, such as in figure 2*b*; a plateau is clearly visible, where the strain increases at constant load. This was very different from the behaviour of normal collagen, which fractured very rapidly after reaching the maximum load (figure 2*a*). The other 8 out of the 20 tendons from the β-APN-treated rats did not show a pronounced plateau, but a load–extension curve typified by figure 2*c*. The tendons from the β-APN-
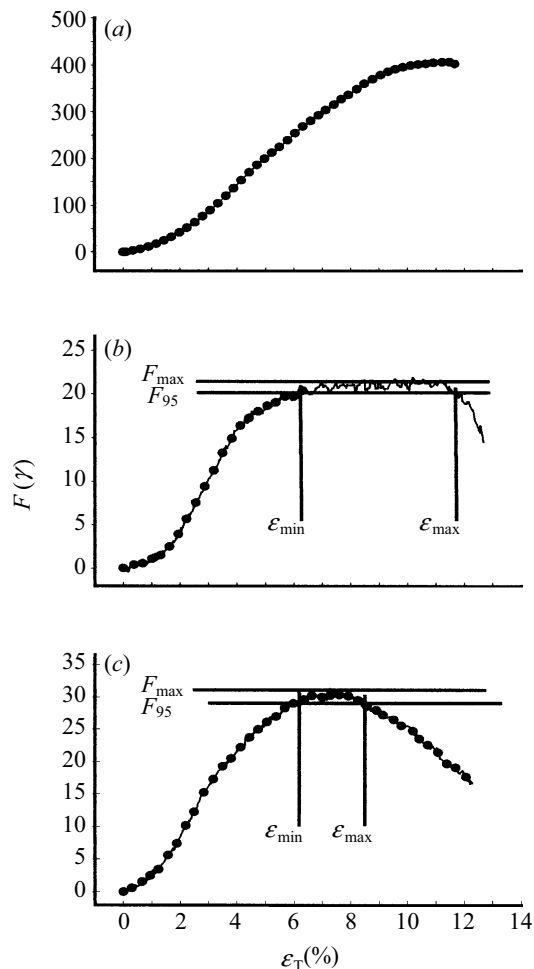
Figure 2. Typical load–extension curves from the rat-tail tendons used in this experiment. The dots represent the mechanical values at the times when an X-ray diffraction pattern was taken. The time needed between two points varied between 30 and 50 s. There were three types of mechanical behaviour: (*a*) the tendons from the normal control group; (*b*) tendons from β-APN-treated rats that showed a marked plateau and (*c*) some β-APN-treated rats that did not show a plateau. A plateau was defined as occurring when the strain at 95% of the maximum load, ε_{max} and ε_{min}, followed the condition $(\varepsilon_{max} - \varepsilon_{min})/\varepsilon_{min} > 0.5$.

treated rats were divided into two groups according to their mechanical behaviour (as in figure 2*b* and *c*, respectively) by estimating the difference between the two strain values, ε_{max} and ε_{min}, measured at 95% of the maximum load (see figure 2*b*,*c*). In cases where (ε_{max} − ε_{min})/ε_{min} was greater than 0.5, the tendon was considered to demonstrate a plateau-like behaviour. No significant effect due to the higher dose of β-APN in one of the animals could be detected.

The applied stress σ is simply the applied force F divided by the cross-sectional area of the tendon. As it was extremely difficult to determine the exact diameter of each tendon, we did not attempt to convert the force–elongation curves into stress–strain curves, thus avoiding the introduction of additional uncertainty into the data. However, it was possible to make a reasonable estimation of the average fracture stress values within the groups because, even though each individual measurement of the
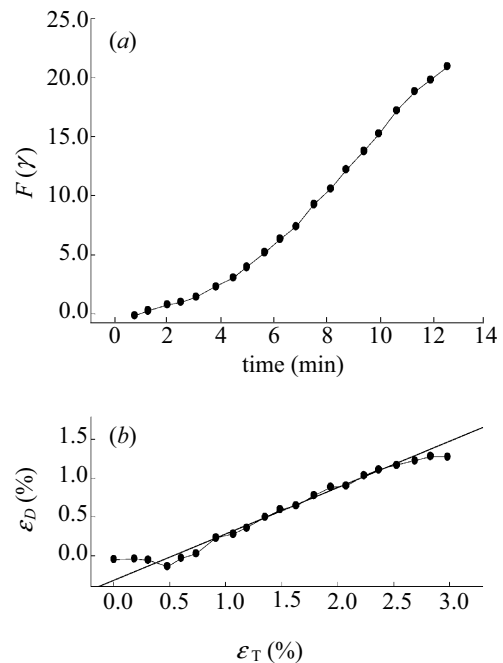

Figure 3. A typical force–elongation curve (*a*) and the corresponding change of the collagen *D*-period, ε_D, as a function of the macroscopic strain of the tendon, ε_T (*b*). In the region where force and elongation were related linearly (curve in *a*), the slope of the graph in *b* was used to determine $d\varepsilon_D/d\varepsilon_T$.

tendon diameter was affected by a large uncertainty, the average value for each group is more reliable. The average maximum force from the control group was *ca.* 390 g, whereas the average failure force of the β-APN-treated samples was *ca.* 28 g. The average diameter of the tendons was *ca.* 200 μm for the controls and *ca.* 150 μm for the β-APN-treated animals. With these values, the average maximum stress of the normal collagen was 120 MPa, whereas the average maximum stress for the β-APN-treated rats was *ca.* 15 MPa, that is, roughly one order of magnitude smaller. The strain at maximum stress was, on average, 6.7% for the β-APN-treated rats and 9.5% for the control group, with a large variation between individual tendons. This means that cross-link-deficient collagen has a dramatically reduced fracture load without a large decrease in extensibility. Axial *D*-periods determined by X-ray diffraction increased between 0.2 and 2 nm before fracture. There was no significant difference in the average values for the β-APN-treated rats (0.81 nm) and the control group (0.87 nm).

The total elongation of the tendons was used to compute the macroscopic strain ε_T, and the change in *D*-period was taken to compute the strain in the fibrils (ε_D) as a function of load within each tendon. The relation between the two strains was analysed in graphs such as those illustrated in figure 3. Using the slope of the plot ε_D versus ε_T in the region where the load–elongation curve was roughly linear, the ratio of fibril to tendon strain, $d\varepsilon_D/d\varepsilon_T$, was determined for each specimen. Figure 4 shows the summary of all values obtained for $d\varepsilon_D/d\varepsilon_T$ as a function of the applied strain rate $d\varepsilon_T/dt$ (*t* being the time). It is clear from figure 4*a* that $d\varepsilon_D/d\varepsilon_T$ increases with strain rate in normal collagen, while it decreases in the
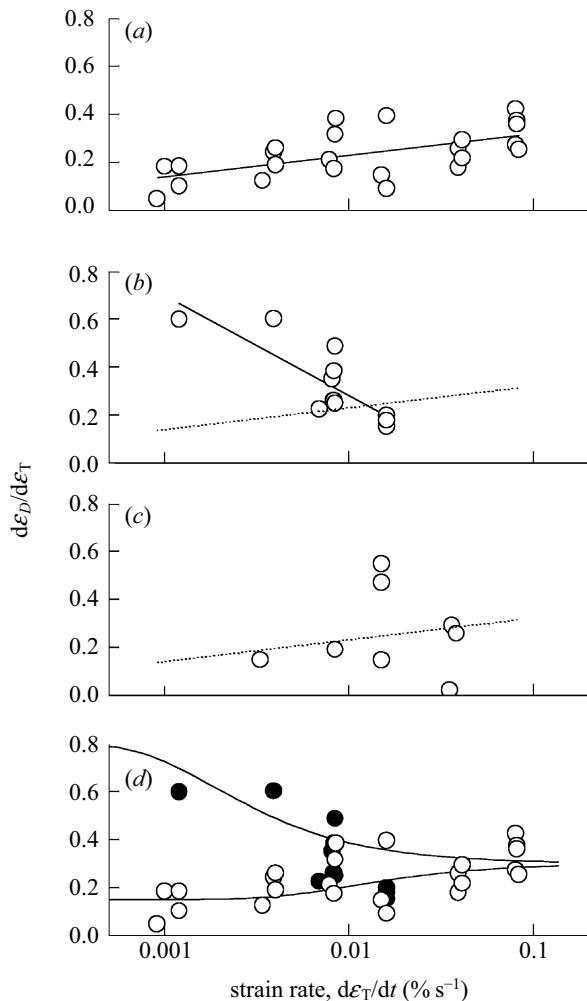
Figure 4. Strain-rate dependency of the ratio of fibril elongation to total tendon elongation $d\varepsilon_D/d\varepsilon_T$, for (a) normal collagen taken from the control group; (b) collagen from β-APN-treated rats that showed a plateau in their force–elongation curves; and (c) collagen from β-APN-treated rats that showed no plateau. The full straight lines in (a) and (b) are the result of linear regression to show the tendency to increase and to decrease with macroscopic strain rate $d\varepsilon_T/dt$, respectively. The dotted lines in (b) and (c) reproduce the regression line from (a) for easier comparison of the data. (d) Compares the data taken from (a) (open circles) and the data from (b) (filled circles) with the model given by equation (A 4). The values chosen for the free parameters in this model are: $\alpha = 0.15$, $\beta = 0.3$, and $\gamma \langle \varepsilon_T \rangle = 0.01$ for the lower curve (normal collagen) and $\alpha^* = 0.8$, $\beta^* = \beta$, $\gamma^* = \gamma\, \alpha/\alpha^*$ for the upper curve (cross-link-deficient collagen).

cross-link-deficient collagen showing a plateau in the force–elongation curve (such as in figure 2b). In normal collagen, the lowest value for $d\varepsilon_D/d\varepsilon_T$ was *ca.* 10% for a strain rate of 0.001% s^{-1} and the highest value was *ca.* 40% at a strain rate of 0.08% s^{-1} (figure 4a). In contrast, the values for 0.0012% s^{-1} were as high as 60% in cross-link-deficient collagen (figure 4b). The data from cross-link-deficient collagen without a plateau scatter considerably (figure 4c) and no clear trend can be seen.

4. DISCUSSION

Simultaneous tensile testing and synchrotron X-ray diffraction characterization investigated the strain-rate dependence of the mechanical properties of rat-tail tendons. The main results can be summarized as follows.

(i) The extension of collagen fibrils inside the tendon is always considerably less than the total extension of the tendon. At slow deformations, this effect is much more pronounced in normal than in cross-link-deficient collagen.

(ii) In normal collagen, the ratio between the extension of the fibrils and of the tendon increases with the strain rate.

(iii) In cross-link-deficient collagen the opposite tendency is observed in connection with the appearance of a plateau in the load–extension curve, indicating pronounced creep behaviour.

(iv) The fracture stress is dramatically reduced (by about a factor of 10) in cross-link-deficient collagen, without a large change in maximum strain.

Clearly, some qualitative conclusions can be drawn from these observations. First, considerable deformation must occur outside the collagen fibrils, presumably in the proteoglycan-rich matrix (observation 1), in agreement with previous work (Fratzl *et al.* 1997). In cross-link-deficient collagen, additional slippage of molecules or subfibril structures (not prevented by covalent cross-linking) may be responsible for the larger relative strain in the fibrils at slow deformation rates. Second, the proteoglycan-rich matrix becomes stiffer when the applied strain rate is larger (observation 2), which is most probably due to a substantial viscous component in its response. Third, the collagen cross-links are crucial in determining the stiffness of the fibrils, since deformation at a given load is much larger in cross-link-deficient than in normal collagen (observation 3), also in agreement with earlier studies (Light & Bailey 1982; Eyre *et al.* 1984; Davison 1989; Lees *et al.* 1990; Bailey *et al.* 1998). Finally, the cross-link deficiency also enhances the creep behaviour of collagen, which further emphasizes the importance of the cross-links for the stability of the tissue. The mechanical behaviour of cross-link-deficient collagen is in this respect somewhat similar to immature collagen, where lower fracture stress and enhanced creep behaviour were also observed (Kastelic & Bear 1980).

Combining the wealth of structural and mechanical information available for the collagen fibril, (Hodge & Petruska 1963; Mosler *et al.* 1985; Folkhard *et al.* 1986; Hulmes *et al.* 1995; Fratzl *et al.* 1993, 1997; Sasaki & Odajima 1996; Misof *et al.* 1997; Sasaki *et al.* 1999), the proteoglycan-rich matrix (Scott 1991; Cribb & Scott 1995), as well as the covalent cross-links (Light & Bailey 1982; Eyre *et al.* 1984; Davison 1989; Lees *et al.* 1990; Bailey *et al.* 1998), we propose a simple model for the strain-rate-dependent effects reported in this paper. This model is illustrated in figure 5. The tendon is considered as a composite material with collagen fibrils embedded in a proteoglycan-rich matrix. This matrix is mostly loaded under shear. Because the spacing between fibrils is much smaller than their length, the shear stress τ effectively
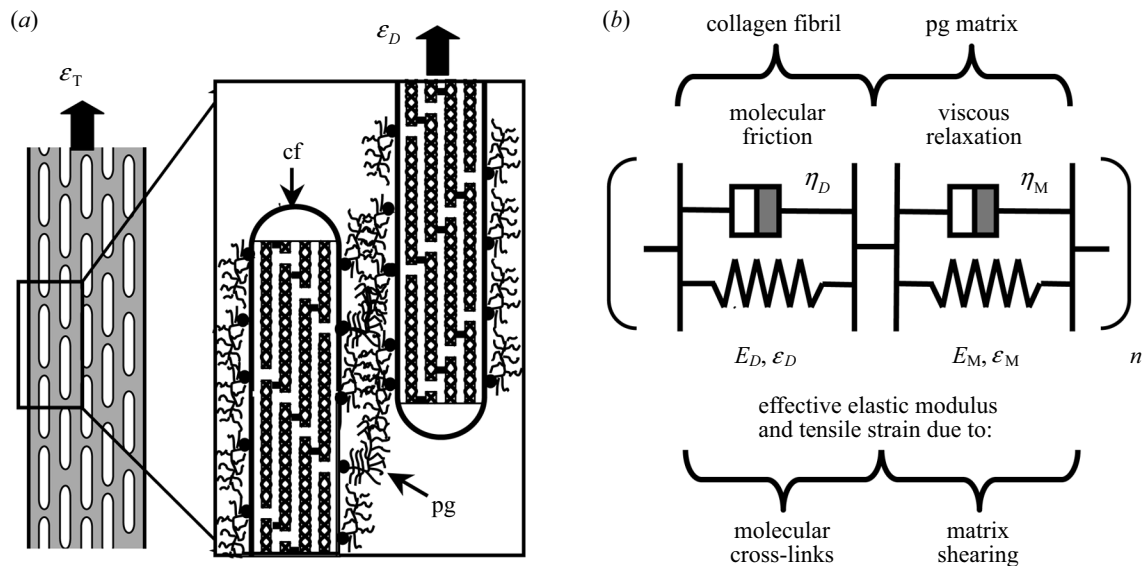
Figure 5. (a) Schematic representation of the hierarchical structure of a collagen tendon. If (a fibre of) the tendon is stretched by an amount ε_T, this is distributed between the collagen fibrils (cf) with a tensile strain ε_D and the proteoglycan-rich matrix (pg), which is mainly sheared. Covalent cross-links between molecules are drawn schematically within the collagen fibrils. (b) An illustration representing a mechanical model, where fibrils and matrix are considered as viscoelastic systems arranged in series. E_D is the elastic modulus of the fibrils that depends critically on the covalent cross-links. η_D is the viscosity of the fibrils, possibly due to friction between molecules. E_M is the effective elastic modulus of the matrix that relates to its shear modulus G by $E_M = G (L/H)^2$, where L is the length and H the lateral spacing between collagen fibrils (Hull 1981; Vincent 1990). The order of magnitude for the length and the diameter of collagen fibrils is 10 and 0.1 μm, respectively. If it is assumed that the lateral distance between fibrils is less than their diameter, then L/H is certainly greater than 100. Finally, η_M is the viscosity of the matrix.

applied to the matrix is much smaller than the tensile stress σ on the tendon. In fact (Hull 1981) $\tau \approx \sigma H/L$, where L is the length of the fibrils and H their spacing. The aspect ratio L/H is typically in the order of 100–1000. One may suppose that the elastic response of the matrix is mostly due to the entanglement of molecules attached to the collagen fibrils, such as proteoglycans. In addition, there will be a considerable viscosity in the matrix due to the many hydrogen bonds that can form in this glassy structure. Although actually deforming in shear, this matrix can mathematically be characterized by an 'effective' elastic modulus E_M (linked to the shear modulus G roughly by $E_M = G (L/H)^2$; Hull (1981); Vincent (1990)) and by the viscosity η_M (figure 5b). In terms of the observed mechanical response when the tendon is stretched, this matrix is effectively in series with the collagen fibrils. The elastic modulus of the fibrils, E_D, is mostly determined by the covalent cross-links and is therefore likely to be considerably decreased in cross-link-deficient collagen. The fibrils will generally also have some viscosity η_D, provided by friction between molecules due to interactions via charges and hydrogen bonds. In total, this provides the very simple model shown in figure 5b.

This viscoelastic model is treated mathematically in Appendix A, where a simple equation is derived for the dependence of $d\varepsilon_D/d\varepsilon_T$ on the strain rate (equations (A 4–A 6)). This model predicts that, at very small strain rates, tendon behaviour is dominated by the elastic moduli, i.e. $d\varepsilon_D/d\varepsilon_T = \alpha = E_M/(E_D + E_M)$, while at large strain rates it is dominated by the viscosity, i.e. $d\varepsilon_D/d\varepsilon_T = \beta = \eta_M/(\eta_D + \eta_M)$. The consequence is that $d\varepsilon_D/d\varepsilon_T$ increases with increasing $d\varepsilon_T/dt$ when α is smaller than β

and decreases in the opposite case. Hence, if in normal collagen $\alpha < \beta$, the behaviour seen in figure 4a is qualitatively reproduced. Furthermore, the cross-link deficiency would decrease E_D and, therefore, increase α. If the increase of α is sufficient, the behaviour of $d\varepsilon_D/d\varepsilon_T$ would be reversed, as illustrated in figure 4b.

In figure 4d, equation (A 4) is plotted with suitably chosen constants (given in Appendix A), together with the data from figure 4a,b. There is a reasonable agreement between the model and the experiments, but this should not be over interpreted since we have no independent estimate of the correct values for the constants α, β and γ. Nevertheless, the model shows that an increase of $d\varepsilon_D/d\varepsilon_T$ with increasing strain rate in normal collagen and a decrease of $d\varepsilon_D/d\varepsilon_T$ with increasing strain rate in cross-link deficient collagen are not unlikely, due to the fact that the mechanical behaviour becomes increasingly dependent on the viscosities when the strain rate increases.

This model relates to the mechanical characteristics of the intact tendon before yielding and failure take place and so does not relate to the different fracture behaviours clearly evident in the right-hand portions of figure 2. Normal rat-tail tendon (figure 2a) normally fails due to fibrils, or groups of fibrils, becoming debonded from the proteoglycan matrix at the maximum load and then pulling out past each other as the load rapidly drops to zero. In normal tendon, the tensile strength of the fibrils greatly exceeds the shear strength of the interface between the fibril and the matrix. In β-APN-treated animals, a proportion of the fibrils have a reduced tensile strength due to reduced cross-link density. This makes it more probable that slippage within fibrils, or groups of fibrils, can occur

while the interface between fibril–fibril group and matrix is still intact. The ultrastructure of the fractured ends of tendons may well reveal clues to such differences in fracture mechanisms and will be investigated further. However, the different mechanical behaviour of the two subgroups identified within the cross-link-deficient tendons (figures 2b and 4b versus figures 2c and 4c) is more difficult to explain. This might possibly be due to the fact that the rats had time to form normal collagen before they were fed with β-APN. It is very probable, therefore, that tendons could contain a mixture of normal and cross-link deficient fibrils. A variation of the relative amounts in this mixture could possibly be the basis of the variations seen in mechanical behaviour. Generally speaking, the properties are more variable in β-APN-fed rats than in normal controls, which is clearly visible from the scattering of the data in figure 4a–c. For a more reliable correlation between cross-links and mechanical properties, one could envisage future work being carried out to measure the cross-link density within each of the tested fibrils. This was beyond the scope of the present study.

The model in figure 5 treats the tendon as a hierarchical level where collagen fibrils and the interfibrillar matrix can be considered as interacting viscoelastic systems. It treats the collagen fibrils as homogeneous entities and neglects the fact that they are assemblies of regularly packed collagen molecules (Hulmes *et al.* 1995). To complete the picture, therefore, figure 6, from a previous publication (Fratzl *et al.* 1997), is included and summarizes all the observations, mostly by *in situ* synchrotron X-ray diffraction, on the deformation mechanisms of normal collagen fibrils (Diamant *et al.* 1972; Mosler *et al.* 1985; Folkhard *et al.* 1986; Sasaki & Odajima 1996; Fratzl *et al.* 1997; Misof *et al.* 1997). This is important since the collagen fibrils experience a significant elongation (given by the strain ε_D), despite the fact that a large fraction of the strain is taken up by the interfibrillar matrix. Depending on the actual strain of the fibril, three mechanisms can be identified: at low strains, a macroscopic crimp of the fibrils is visible in polarized light (figure 6a) is removed (Diamant *et al.* 1972) and subsequently the lateral order of the collagen molecules increases (figure 6b), which was interpreted as a straightening of kinked molecules (Misof *et al.* 1997). Finally, the straight section of the stress–strain curve corresponds to a side-by-side gliding of the molecules, which changes the axial packing of the tendon (Folkhard *et al.* 1986; Fratzl *et al.* 1997; Misof *et al.* 1997). In addition, the triple-helical molecules can also be slightly stretched, leading to a change of the helix pitch (Mosler *et al.* 1985; Sasaki & Odajima 1996).

In conclusion, the complex viscoelastic behaviour of collagen cannot be understood without considering the hierarchical nature of the structure. Indeed, a number of different deformation mechanisms operate at the various levels providing collagen with its remarkable strength and tensile stiffness.

APPENDIX A: VISCOELASTIC MODEL

The interacting systems of the fibrils and the matrix within a collagen fibre can be mechanically described by
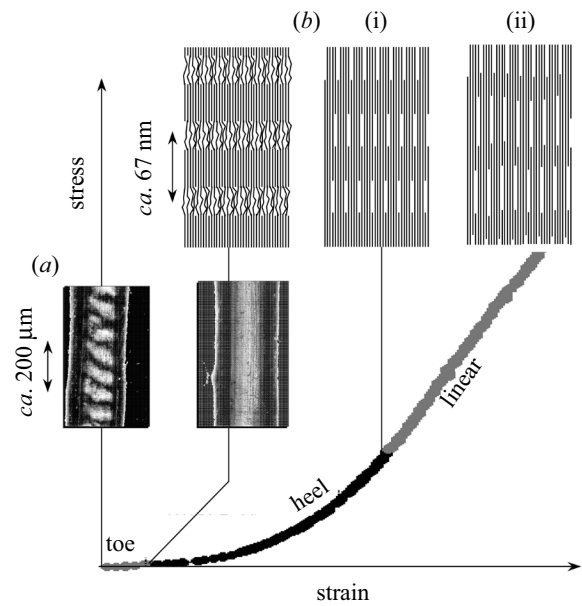
Figure 6. Schematic behaviour of the normal collagen fibril structure from rat-tail tendon (marked cf in figure 5) during tensile deformation (from Fratzl *et al.* 1997). The experiment was performed at a strain rate where the actual strain of the fibril (ε_D) was *ca.* 40% of the total strain of the tendon (ε_T) in the linear region. The total strain of the tendon (ε_T) is plotted on the horizontal axis. Previous synchrotron X-ray scattering experiments (Misof *et al.* 1997) have shown that the tendon structure goes through a sequence of changes upon stretching. First, a macroscopic crimp in the tendon (Diamant *et al.* 1972) is straightened out, as visible in the polarized light (*a*). Then microscopic kinks in the collagen molecules (located mostly in the gap region of the fibril structure) are removed, leading to an entropic contribution to elasticity (*b*(i)). Finally the molecules start to glide past each other in the linear region of the stress–strain curve (*b*(ii)).

two so-called Kelvin models in series, as seen in figure 5b. One Kelvin model stands for the matrix and one for the fibrils. As the same stress acts on both systems, they are put into series.

From the mechanical equilibrium follows

$$\eta_D \dot{\varepsilon}_D + E_D \varepsilon_D = \eta_M \dot{\varepsilon}_M + E_M \varepsilon_M, \qquad (A\,1)$$

where the dot represents the time derivative. The various quantities are defined in figure 5 and the subscripts M and D designate the molecule and the fibril, respectively. The macroscopic strain is defined by

$$(\varepsilon_D + \varepsilon_M) = \varepsilon_T = \dot{\varepsilon}_T^* t, \qquad (A\,2)$$

where t is the time and the strain rate $\dot{\varepsilon}_T$ is constant during the tensile test. This system of differential equations can easily be solved and one obtains

$$\varepsilon_D = \alpha \varepsilon_T + (\beta - \alpha)(1 - e^{-\gamma \varepsilon_T / \dot{\varepsilon}_T}) \dot{\varepsilon}_T / \gamma, \qquad (A\,3)$$

and, consequently (using $\dot{\varepsilon}_T$ as a constant)

$$d\varepsilon_D / d\varepsilon_T = \alpha + (\beta - \alpha) e^{-\gamma \varepsilon_T / \dot{\varepsilon}_T}, \qquad (A\,4)$$

where we have defined:

$$\alpha = \frac{E_M}{E_D + E_M}; \;\; \beta = \frac{\eta_M}{\eta_D + \eta_M}; \;\; \gamma = \frac{E_D + E_M}{\eta_D + \eta_M}. \qquad (A\,5)$$

Equation (A 4) defines $d\varepsilon_D/d\varepsilon_T$ as a function of the strain rate, which corresponds exactly with the curve in figure 5. The constants α, β, and γ define the mechanical properties of collagen fibrils and the interfibrillar matrix. ε_T in equation (A 4) is the typical value of the strain where $d\varepsilon_D/d\varepsilon_T$ was determined. This was of the order of a few percentage points in all fibrils, and one may assume $\varepsilon_T = \langle \varepsilon_T \rangle = \text{constant}$ in equation (A 4).

Assuming, further, that the β-APN treatment changes only the elastic modulus of the fibrils from E_D to a smaller value E_D^* (due to fewer covalent cross-links), then the corresponding constants for the β-APN-treated animals relate to the normal values by:

$$\alpha^* = \frac{E_M}{E_D^* + E_M}; \ \beta^* = \beta; \ \gamma^* = \gamma\alpha/\alpha^*. \tag{A 6}$$

Equation (A 4) was plotted in figure 4*d* for the following two sets of values:

(i) $\alpha = 0.15$; $\beta = 0.3$, $\gamma \langle \varepsilon_T \rangle = 0.01\%\ \mathrm{s}^{-1}$, for the normal tendon;
(ii) $\alpha^* = 0.8$, the values of β^* and γ^* following from equation (A 6), for the β-APN-treated animals.

REFERENCES

Amenitsch, H., Bernstorff, S. & Laggner, P. 1995 High flux beamline for small-angle X-ray scattering at ELETTRA. *Rev. Sci. Instrum.* **66**, 1624–1626.

Bailey, A. J., Paul, R. G. & Knott, L. 1998 Mechanisms of maturation and ageing of collagen. *Mechanisms Ageing Dev.* **106**, 1–56.

Cribb, A. M. & Scott, J. 1995 Tendon response to tensile stress: an ultrastructural investigation of collagen: proteoglycan interactions in stressed tendon. *J. Anat.* **187**, 423–428.

Davison, P. F. 1989 The contribution of labile crosslinks to the tensile behavior of tendons. *Connect. Tiss. Res.* **18**, 293–305.

Diamant, J., Keller, A., Baer, E., Litt, M. & Arridge, R. G. C. 1972 Collagen: ultrastructure and its relation to mecahnical properties as a function of aging. *Proc. R. Soc. Lond.* B **180**, 293–315.

Eyre, D. R., Paz, M. A. & Gallop, P. A. 1984 Crosslinking in collagen and elastin. *A. Rev. Biochem.* **53**, 717–748.

Folkhard, W., Mosler, E., Gercken, W., Knörzer, E., Nemet-schek-Gansler, H., Nemetschek, T. & Koch, M. H. J. 1986 Quantitative analysis of the molecular sliding mechanism in native tendon collagen—time resolved dynamic studies using synchrotron radiation. *Int. J. Biol. Macromol.* **9**, 169–175.

Fratzl, P., Fratzl-Zelman, N. & Klaushofer, K. 1993 Collagen packing and mineralization: an X-ray scattering investigation of turkey leg tendon. *Biophys. J.* **64**, 260–266.

Fratzl, P., Misof, K., Zizak, I., Rapp, G., Amenitsch, H. & Bernstorff, S. 1997 Fibrillar structure and mechanical properties of collagen. *J. Struct. Biol.* **122**, 119–122.

Hodge, A. J. & Petruska, J. A. 1963 Recent studies with the electron microscope on ordered aggregates of the tropocollagen molecule. In *Aspects of protein structure*, pp. 289–308. London: Academic.

Hull, D. 1981 *An introduction to composite materials.* Cambridge University Press.

Hulmes, D. J. S., Wess, T. J., Prockop, D. J. & Fratzl, P. 1995 Radial packing, order and disorder in collagen fibrils. *Biophys. J.* **68**, 1661–1670.

Kastelic, J. & Baer, E. 1980 Deformation in tendon collagen. *Proc. 34th Symp. Soc. Exp. Biol.* **34**, 397–435.

Lees, S., Eyre, D. R. & Barnard, S. M. 1990 β-APN dose dependence of mature crosslinking in bone matrix collagen of rabbit compact bone: corresponding variation on sonic velocity and equatorial diffraction spacing. *Connect. Tiss. Res.* **24**, 95–105.

Light, N. D. & Bailey, A. J. 1982 Covalent cross-links in collagen. In *Meth. Enzymol.* **82A**, 360–372.

Misof, K., Rapp, G. & Fratzl, P. 1997 A new molecular model for collagen elasticity based on synchrotron radiation evidence. *Biophys. J.* **72**, 1376–1381.

Mosler, E., Folkhard, W., Knörzer, E., Nemetschek-Gansler, H. & Koch, M. H. J. 1985 Stress induced molecular rearrangement in tendon collagen. *J. Mol. Biol.* **182**, 589–596.

Sasaki, N. & Odajima, S. 1996 Elongation mechanism of collagen fibrils and force-strain relations of tendon at each level of structural hierarchy. *J. Biomech.* **29**, 1131–1136.

Sasaki, N., Shukunami, N., Matsushima, N. & Izumi, Y. 1999 Time resolved X-ray diffraction from tendon collagen during creep using synchrotron radiation. *J. Biomech.* **32**, 285–292.

Scott, J. E. 1991 Proteoglycan: collagen interactions in connective tissues. Ultrastructural, biochemical, functional and evolutionary aspects. *Int. J. Biol. Macromol.* **13**, 157–161.

Tang, S., Trackman, P. C. & Kagan, H. M. 1983 Reaction of aortic lysyl oxidase with β-aminopropionitrile. *J. Biol. Chem.* **10**, 4331–4338.

Vincent, J. 1990 *Structural biomaterials.* Princeton University Press.